Heterogeneous Kinetics of the Uptake of HOBr on Solid Alkali Metal Halides at Ambient Temperature †

ARTICLE *in* THE JOURNAL OF PHYSICAL CHEMISTRY A · JUNE 1998

Impact Factor: 2.69 · DOI: 10.1021/jp980849q · Source: OAI

4 AUTHORS, INCLUDING:

Michihiro Mochida
Nagoya University
62 PUBLICATIONS **1,766** CITATIONS
SEE PROFILE

Hajime Akimoto
National Institute for Environmental Studies
341 PUBLICATIONS **10,762** CITATIONS
SEE PROFILE

Michel J Rossi
Paul Scherrer Institut
261 PUBLICATIONS **6,403** CITATIONS
SEE PROFILE

Heterogeneous Kinetics of the Uptake of HOBr on Solid Alkali Metal Halides at Ambient Temperature†

M. Mochida,‡,§ H. Akimoto,‡ H. van den Bergh,§ and M. J. Rossi*,§

Research Center for Advanced Science and Technology, University of Tokyo, 4-6-1 Komaba, Meguro-ku, Tokyo 153, Japan, and Laboratoire de Pollution Atmosphérique et Sol (LPAS), Swiss Federal Institute of Technology (EPFL), CH-1015 Lausanne, Switzerland

Received: January 22, 1998; In Final Form: March 25, 1998

The heterogeneous reactions of HOBr with solid crystalline NaCl [HOBr(g) + NaCl(s) → BrCl(g) + NaOH-(s)] and KBr [HOBr(g) + KBr(s) → Br_2(g) + KOH(s)] substrates at ambient temperature have been investigated using a Teflon coated Knudsen cell reactor. Powder, grain, and spray-deposited salt substrates were used for the measurement of the HOBr reactivity. The observed uptake probability depends on the total external surface area of the salt substrates. For NaCl substrates, Br_2 and BrCl are observed as products; for KBr substrates, Br_2 is observed as the sole product. In both cases, a dependence of the initial uptake probability γ_0 on HOBr flow rate has been observed. The initial uptake is large at low flow rate and 10 times smaller at high flow rate. Values of $\gamma_0 \leq (6.5 \pm 2.5) \times 10^{-3}$ for NaCl and $\gamma_0 \leq 0.18 \pm 0.04$ for KBr are obtained under our experimental conditions of limiting low flow rates akin to atmospheric conditions. The production of Br_2 is observed even for HOBr interacting on solid $NaNO_3$, a non-halogen containing substrate. The yield measurements imply that a HOBr self-reaction occurs on salt surfaces according to $2HOBr \rightarrow Br_2 + H_2O + {}^1/_2O_2$. The decrease in Br_2 yield with increasing HOBr flow rate from 100 to 50% indicates that a competition between the heterogeneous reaction of HOBr with NaCl or KBr and the self-reaction of HOBr takes place on the solid salt surface under laboratory experimental conditions. The decrease of γ_0 with time indicates that approximately 5−10% of the Br atoms on a KBr surface interact with HOBr.

Introduction

Bromine containing compounds are thought to play an important role in the ozone destruction in various regions of the atmosphere. Barrie et al.[1] first reported a relationship between springtime ozone depletion in the lower Arctic troposphere which shows a strong negative correlation between the concentration of ozone and bromine compounds. This phenomenon has been reconfirmed in subsequent field measurements,[2−6] and heterogeneous reactions on sea salt particles have been invoked as potential sources of photoactive bromine compounds which cause ozone destruction. From kinetic studies of heterogeneous reactions on salt particles, a few key reactions have been proposed in order to rationalize the Br sources and the cycling of bromine species.[7−21]

Recent studies of atmospheric bromine chemistry suggest that HOBr is one of the important bromine compounds.[22−25] The rapid photolysis of HOBr in daytime releases bromine atoms and hydroxyl radicals, which causes ozone destruction according to the reactions in eqs 1−5.

$$Br + O_3 \rightarrow BrO + O_2 \quad (1)$$

$$HO_2 + BrO \rightarrow HOBr + O_2 \quad (2)$$

$$HOBr + h\nu \rightarrow OH + Br \quad (3)$$

$$OH + O_3 \rightarrow HO_2 + O_2 \quad (4)$$

net:
$$2O_3 \rightarrow 3O_2 \quad (5)$$

In addition to the ozone destruction mechanism written in eqs 1−5, another mechanism involving the heterogeneous reaction in or on liquid aerosols is also proposed:

$$BrONO_2 + H_2O \xrightarrow[\text{het.}]{} HOBr + HNO_3 \quad (6)$$

Because of the recent attention to HOBr, several measurements of HOBr properties have been reported: for example, ideal gas thermodynamic properties,[26] UV/visible absorption spectra,[27] near-threshold photodissociation dynamics,[28] and an ab initio study of the electronic absorption spectrum.[29]

Regarding the heterogeneous reaction of HOBr, Abbatt and Oppliger et al. have reported the HOBr reaction with ice[30,31] and supercooled sulfuric acid solution.[32] Kirchner et al. reported the HOBr reaction on an ice surface doped with sea salt.[33] However, experimental studies of the HOBr heterogeneous reaction on solid salt surfaces have not been reported. Salt particles exist in the marine boundary layer, in the stratosphere after volcanic eruption,[34] and in plumes from burning oil wells.[35−37] Although salt particles most often occur as solution droplets in the marine boundary layer, some of these particles may be transported to a dry atmosphere where they are found as solid crystalline salt particles.[38] In this study, the reactivity of HOBr with solid alkali metal halides is reported which affords insights into the importance of heterogeneous reactions of HOBr with salt. In addition, emphasis is placed on mechanistic aspects of the heterogeneous reaction in order to be able to extrapolate the kinetics to environmental conditions with confidence.

Experimental Section

The experiments have been performed using a Knudsen cell reactor shown in Figure 1, which consists of a Knudsen reactor coupled to a differentially pumped quadrupole mass spectrometer (Balzers model QMG 421). A detailed description of this

* To whom correspondence should be addressed.

† Experimental work carried out at EPFL under the auspices of the Alliance for Global Sustainability (AGS).

‡ University of Tokyo.

§ Swiss Federal Institute of Technology (EPFL).

S1089-5639(98)00849-4 CCC: $15.00
Published on Web 06/02/1998

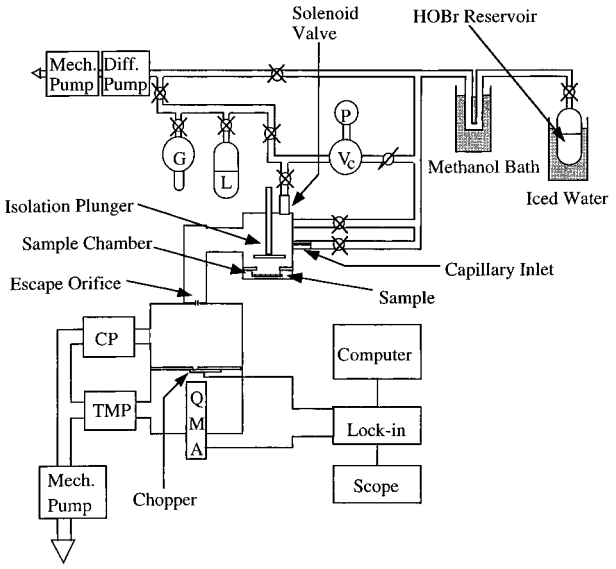

Figure 1. Schematic drawing of the experimental apparatus. The upper part represents the gas handling system. The Knudsen cell is mounted on a differentially pumped vacuum chamber; the upper chamber is pumped by a cryopump (CP) and the lower chamber by a turbomolecular pump (TMP). The gas species are detected by a quadrupole mass spectrometer (QMA).

TABLE 1: Knudsen Cell Parameters

reactor parameter	value
volume	1830 cm^3
estd surface area (total)	1300 cm^2
surface area (sample)	19.6 cm^2
gas number density	$(1-100) \times 10^9$ cm^{-3} [a]
sample collision freq[b]	$\omega = 2.0A_h(T/M)^{1/2}$ s^{-1}
escape rate constant ($\phi = 14$ mm)[c]	$1.8 \times (T/M)^{1/2}$ s^{-1}

[a] Calculated using the relation $F^i = Vk_{esc}[M]$, where F^i is the flow of molecules, V the reactor volume, and [M] the number density. [b] A_h, the sample surface area. [c] Value determined directly by experiment.

reactor is presented elsewhere.[39,40] The pressure inside the reactor is kept at molecular flow conditions. The inner wall of the reactor has been coated with Teflon (Dupont, FEP 120 suspension) in order to minimize adsorption and catalytic reaction of gas species. In our measurements, the effects of the wall reaction inside the Knudsen reactor was negligible compared to the reactivity of the salt surface. The introduction of the gaseous species onto the salt surface is controlled by use of an isolation plunger. The gaseous species effuse from the reactor to the mass spectrometer in a molecular beam which is chopped at 70 Hz and detected by an electron impact quadrupole mass spectrometer (MS). The modulated electron multiplier signal is lock-in amplified by a digital lock-in amplifier (Stanford Research SRS830 DSP).

The HOBr flow inside the reactor was varied between 10^{13} and 10^{15} molecules s^{-1}, corresponding to a concentration range between 10^9 and 10^{11} molecules/cm^3. The residence time of HOBr in the reactor was set by the size of the escape orifice which formed the exit of the Knudsen cell reactor sitting atop the differentially pumped chamber housing the mass spectrometer. We could choose from 1, 4, 8, and 14 mm diameter orifice sizes for the present experiments. For most of the HOBr experiments reported herein the 14 mm orifice is used. Characteristic parameters of our Knudsen cell reactor are presented in Table 1.

We used commercial NaCl (Fluka puriss. p.a.) and KBr (Fluka puriss. p.a. ACS) for this study. Two types of salt samples, namely, powder substrates and spray-deposited substrates, were prepared for these experiments. Powder substrates were obtained by grinding the salt in a ball mill. Average diameters of the powder particles were approximately between 10 and 100 μm.

Spray-deposited salt substrates were prepared as follows: a saturated salt solution in methanol was sprayed using a capillary-source atomizer onto 50 mm diameter glass optical flats heated to a temperature of 420 K. The solvent immediately evaporated, and the salt formed a coherent film across the surface of the glass flat as measured by a profilometer. It is known from SEM measurements that the total exposed surface is nearly equivalent to the area of the coated flat.[14] Typically, several milligrams of salt were deposited onto the glass flats, resulting in an average thickness of several micrometers.

Two types of experiments have been performed: steady-state and pulsed valve experiments. In steady-state experiments, the uptake probability is determined by measuring the steady-state MS signal with the sample isolated and exposed, respectively. These signals are then used to calculate the pseudo-first-order loss rate constant of the gas, k_{uni}, according to the relation:

$$k_{uni} = \left(\frac{S_i}{S_f} - 1\right)k_{esc} \tag{7}$$

where S_i and S_f refer to the MS signals before and during reaction and k_{esc} is the rate constant for the effusive loss from the reactor which depends on the orifice size. Because the use of large orifices leads to a discrepancy between the measured k_{esc} and the ones calculated using gas kinetic theory, measured values of k_{esc} for HOBr are used throughout. The values of k_{esc} presented in Table 1 agree well with those obtained for other gases such as He, O_2, and N_2. The uptake probability γ is calculated according to

$$\gamma = k_{uni}/\omega \tag{8}$$

where ω is the calculated collision frequency of the average molecule with the geometrical surface of 19.6 cm^2. When using powder substrates, it is necessary to take into account the total exposed surface area and morphology. Keyser et al. have proposed a model[41-45] originally developed by Wheeler and others[46,47] in which the overall rate of uptake can be separated into diffusional and reactive components. Correction factors are calculated, and the observed uptake probability γ_{obs}, which is the value measured when the powder substrates are regarded as perfectly flat geometric and thus structureless surfaces, can be converted to the true uptake probability γ_{tr} on a per collision basis. Our recent experiments indicate that there are two types of reactions concerning the gas uptake on salt systems.

We have observed that reactions of N_2O_5 on salt[14] showed good agreement with the predictions of this pore diffusion model, whereas HNO_3 does not show diffusion into the internal voids of the sample represented as straight cylindrical pores in the model of Keyser et al. This was explained by the fact that "sticky" molecules such as HNO_3 do not diffuse across the top layer and therefore do not interact with the underlying internal surface area.[11] Thus, they interact only with the apparent geometrical surface of the sample. Figure 2 shows the dependence of the measured uptake rate of HOBr as a function of the sample mass determined in steady-state experiments on NaCl powder of controlled particle size. These monodisperse grain samples have been prepared by grinding salt in a ball mill and sieving in order to isolate a specific size fraction. As a result salt grains with characteristic dimensions in the range 350−500 μm are obtained. The pore diffusion model is

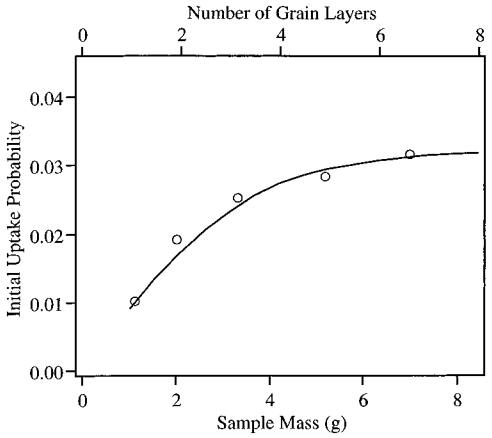

Figure 2. Mass dependence of the HOBr initial uptake coefficient on the mass of NaCl monodisperse grain (dimension in the range of 350−500 μm). Each value of γ_{obs} has been obtained at a HOBr flow of 5.8 $\times$ 10^{13} molecules/s. The solid curve represents the theoretical value according to the model presented by Keyser et al. The "true" value of the uptake probability, γ_{tr}, is 2.8 $\times$ 10^{-3}.

subsequently applied using the known true density ρ_t, the volumetrically measured apparent bulk density (ρ_b) of the salt grains at hand, and the "tortuosity factor" τ fixed at a value of 2.0 as input parameters. The parameter τ is an empirical correction for the fact that the random grain packing leads to irregular pores as opposed to regular ones assumed in the model. The true uptake coefficient γ_{tr} is subsequently treated as the only variable fit parameter to the sample mass dependence of γ_{obs} such as displayed in Figure 2. It also is apparent that the observed uptake probability γ_{obs} is increasing with sample mass, reflecting the increase of the total sample surface area interacting with the gaseous reactant with increasing sample mass. The increase of γ_{obs} saturates at large sample mass because the number of layers exceeds the depth of diffusion of gas into the internal voids. For HOBr interacting with KBr powder the dependence of γ_{obs} on sample mass has been observed as well. Thus, for the study of HOBr uptake on solid NaCl and KBr salt, the true uptake probability γ_{tr} has been obtained by fitting it to the observed values of γ_{obs} as a function of sample mass.

A typical pulsed valve experiment is carried out by introducing the gaseous reactant through a solenoid valve in millisecond pulses. It corresponds to a real-time kinetics experiment. First, the reactant gas is introduced while the isolation plunger is lowered; thus, the sample chamber closed. The MS signal of the gaseous reactant shows an exponential decay which corresponds to k_{esc} (cf. Figure 3b). Subsequently a second pulse is fired with the isolation plunger lifted; thus, the sample chamber is exposed to HOBr. The MS signal shows a faster decay which corresponds to the sum of $k_{esc} + k_{uni}$. At last, the MS detection is switched to the expected products. These MS signals usually have a peak occurring at some time delay compared to the time dependent MS signal of the reactant. The pulsed valve experiments reveal the mechanism of the reaction, the extent to which the products interact with the salt surface, and the mass balance of the reaction.

HOBr was synthesized by slowly dripping Br_2 into an aqueous $AgNO_3$ solution. The so produced HOBr in solution was distilled under reduced pressure and collected in a 30 wt % H_2SO_4 solution kept at −50 °C and stored at dry ice temperature in order to prevent decomposition of the dissolved HOBr. For the uptake experiments, the H_2SO_4 solution containing HOBr was warmed to 0 °C and the HOBr gas evaporating from the solution trapped in a Teflon coil at −70 °C and introduced into

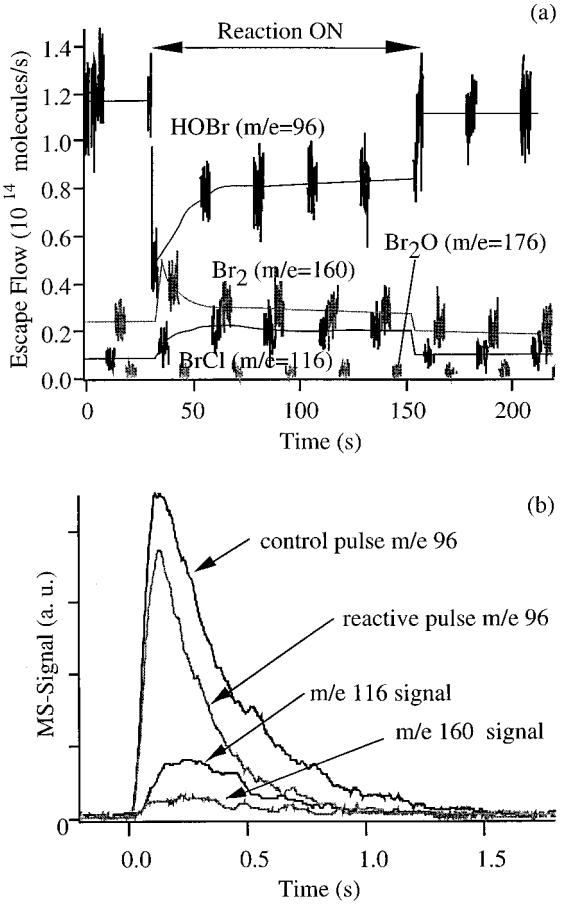

Figure 3. (a) Steady-state experiment for a typical HOBr reactive uptake on NaCl powder. The HOBr flow rate of 1 $\times$ 10^{14} molecules/s is monitored at *m/e* 96, Br_2 at *m/e* 160, BrCl at *m/e* 116, and Br_2O at *m/e* 176 in the 14 mm orifice reactor. (b) Pulsed-valve experiment of HOBr on NaCl powder substrate. The *m/e* 96 signal of the "control pulse" is obtained with the isolation plunger lowered and the 14 mm orifice reactor; the "reactive pulse", with the plunger lifted. The product signals are recorded at *m/e* 116 and *m/e* 160.

the Knudsen reactor by controlling the temperature of the Teflon coil trap. The main contaminants of HOBr were Br_2 and Br_2O, which were controlled at less than 5% of the amount of HOBr by adjusting the temperature of the trap.

The calibration of the MS signals to partial pressure in the Knudsen cell was performed in the following way. For gases without significant contamination such as Br_2, the sample was filled into a known storage volume which is connected to the Knudsen reactor by a capillary. The flow of the gas into the Knudsen cell gives rise to a decrease of the pressure in the storage volume and is accompanied by the appearance of a MS signal of the gas effusing from the Knudsen reactor. The flow rate is calculated from the rate of pressure change. Thus, the conversion factor between the intensity of the MS signals and the flow rate can be obtained. However, the absolute calibration of the MS signal intensity of HOBr has been obtained by using a relative method which was put later on an absolute basis. It was performed by using the following reactions on ice surfaces:[31]

$$HOBr + HCl \rightarrow BrCl + H_2O \quad (9)$$

$$HOBr + HBr \rightarrow Br_2 + H_2O \quad (10)$$

These heterogeneous reactions are quite rapid at excess HCl and HBr, and yields of 100% for Br_2 and BrCl are obtained.

Two consecutive calibrations using the above two reactions show good agreement with a discrepancy between them of approximately 5%. The yield measurements of HOBr also support the accuracy of these calibrations (discussed below).

HOBr stored in the trap by the method described above contains some amount of Br_2O because of the rapid establishment of the following equilibrium:

$$Br_2O + H_2O \leftrightarrows 2HOBr \qquad (11)$$

To reduce the amount of Br_2O contained in the HOBr source, the cold trap holding the HOBr must contain some ice. This in turn causes contamination of the HOBr with H_2O vapor.

To apply obtained uptake probabilities to atmospheric conditions, the rate of loss of HOBr is not only controlled by γ_{tr}. The flow J_c (molecules s^{-1}) of HOBr to aerosol particles may be rate-controlling because it is limited by gas-phase diffusion and is expressed in eq 12, where R_p is the radius of the particle,

$$J_c = 4\pi R_p D(c_\infty - c_s)\beta \qquad (12)$$

D is the molecular diffusivity, c_∞ and c_s are the concentrations of reactant at infinity and at the aerosol surface, and β is a conversion factor which is given by eq 13.[48] In eq 13, Kn_D is

$$\beta = \frac{1 + Kn_D}{1 + 2Kn_D(1 + Kn_D)/\alpha} \qquad (13)$$

the Knudsen number and α is the mass accommodation coefficient. This value for β is quite sensitive to the uptake probability when the diameter of the aerosol is small. It is reported that sea salt particles range from 0.02 to 60 μm in diameter.[49] For large aerosol particles of 10 μm or so in diameter, the rate of HOBr uptake will be limited by gas-phase diffusion and the value of the uptake coefficient will influence the rate of uptake only to a minor extent. The other extreme is represented by aerosol diameters less than 0.1 μm or so for which Kn_D is large. In this case effective molecular flow conditions prevail such that gas-phase diffusion becomes unimportant and the rate of uptake is entirely controlled by the magnitude of γ_{tr}. We would like to stress that the Knudsen cell technique is well-suited to the measurement of large uptake coefficients because of the absence of a carrier gas which may impose significant limitations on the measurement of the uptake rate because of slow gas-phase diffusion relative to the rate of uptake.

Results and Discussion

Figure 3 shows a typical HOBr reactive uptake experiment on a NaCl substrate in a steady-state experiment (a) and in a pulsed-valve experiment (b). In the steady-state experiment shown in Figure 3a, it can be seen that the HOBr partial pressure monitored at *m*/*e* 96 which is proportional to the flow of HOBr out of the reactor (see footnote *a* to Table 1 for the conversion) readily drops after the plunger is lifted. The HOBr flow monitored at *m*/*e* 96 will eventually reach the initial level of the flow present before the interaction with the sample. This behavior corresponds to gradual saturation of the HOBr uptake until complete saturation (not shown) and suggests that the nature of the surface changes owing to deactivation. Accompanied by HOBr uptake on NaCl, the products BrCl (*m*/*e* 116) and Br_2 (*m*/*e* 160) have been observed. Upon lifting the plunger, Br_2 immediately appears, apparently resulting from the fast initial uptake rate of HOBr. On the other hand, the appearanceof BrCl is delayed and the BrCl signal reaches its maximum value several tens of seconds after the sample chamber is opened. Figure 3b shows an example of a pulsed-valve experiment. The "control pulse" at *m*/*e* 96 with the isolation plunger lowered shows an exponential decay whose rate corresponds to k_{esc}, whereas "reactive pulse" with the plunger lifted shows a faster decay owing to the uptake of HOBr on NaCl substrates. In contrast to the results of steady-state experiments, pulsed-valve experiments show that MS signals of both Br_2 and BrCl have peaks approximately 100 ms after HOBr injection. Thus, the gradual appearance of BrCl in steady-state experiments must be due to a change in the branching ratio of Br_2 to BrCl brought about by changing surface conditions. A change of the concentration of HOBr adsorbed on the surface with time may affect this ratio because the self-reaction of HOBr results in Br_2 as discussed below. The expected heterogeneous reaction is

$$HOBr(g) + NaCl(s) \rightarrow BrCl(g) + NaOH(s) \qquad (14)$$

which releases BrCl from the NaCl surface. As Br_2 is an unexpected product, it may originate from the bimolecular self-reaction of HOBr discussed in more detail below. Another possibility for formation of Br_2 is reaction 15, which is a

$$HOBr(g) + BrCl(g) \rightarrow HOCl(g) + Br_2(g) \qquad (15)$$

secondary reaction to reaction 14. However, we did not observe HOCl at *m*/*e* 52 which, if formed, should be observable by virtue of the fact that HOCl did not react on NaCl samples under our experimental conditions. Therefore, we rule out reaction 15 as a molecular bromine generator.

A typical HOBr reactive uptake experiment on a KBr substrate in a steady-state and pulsed-valve experiment are presented in Figure 4a,b. Br_2 has been observed as the unique product in our experiments. The expected reaction is

$$HOBr(g) + KBr(s) \rightarrow Br_2(g) + KOH(s) \qquad (16)$$

Similar to the HOBr reaction with NaCl, a variable amount of Br_2 may come from the self-reaction of HOBr on the salt surface depending on the flow rate of HOBr. It has to be noted that the condensed-phase products NaOH(s) and KOH(s) in eqs 14 and 16, respectively, have not been directly observed in the present experiments. They are specified in order to balance the stoichiometry of the reaction.

Uptake Probabilities. For the HOBr reactions with NaCl and KBr, the dependence of the HOBr uptake probability on the HOBr flow rate is shown in Figure 5. Each plot represents the initial uptake probability on a "virgin" salt sample which is exposed to HOBr for the first time.

For NaCl, spray-deposited substrates could not be used for measuring the uptake probability of HOBr because it is not sufficiently large to measure the difference of the MS signals before and during reaction if the 14 mm orifice is used. Usually the most convenient way to measure a small uptake probability is to use a small orifice size. In this case, however, the increase in the pressure inside the Knudsen reactor caused by using a small orifice size exceeded the range for the validity of the molecular flow regime. As described above, the results obtained on powder substrates or salt grains are converted using the pore diffusion model presented in the Experimental Section. For KBr substrates, both spray-deposited substrates and powder substrates are used in order to determine the uptake probability. The results obtained by using powder substrates are also corrected for pore diffusion. These two independent data sets derived

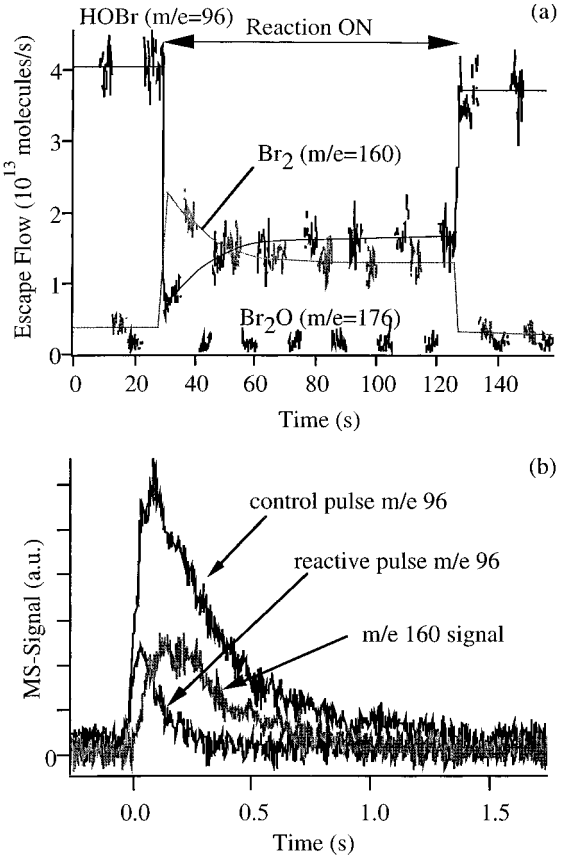

Figure 4. (a) Steady-state experiment for a typical HOBr reactive uptake on KBr powder. The HOBr flow rate of 4×10^{13} molecules/s is monitored at *m/e* 96, Br_2 at *m/e* 160, BrCl at *m/e* 116, and Br_2O at *m/e* 176 in the 14 mm orifice reactor. (b) Pulsed-valve experiment of HOBr on KBr powder substrate using the 14 mm orifice reactor. The *m/e* 96 signal of the "control pulse" is obtained with the isolation plunger lowered; the "reactive pulse", with the plunger lifted. The product signal is recorded at *m/e* 160 (Br_2).

on one hand from the results on spray-deposited and on the other hand on powder substrates show good agreement and thus give us confidence in our method of finding the true uptake probability. Values of uptake probabilities are shown in Tables 2 and 3.

In both cases, the uptake probabilities are relatively high at low flow rate, that is, at low HOBr partial pressure in the Knudsen reactor, and low at high flow rates as shown in Figure 5a,b. Thus, the HOBr−salt interaction does not obey a first-order kinetic law for adsorption which has been observed for other salt reactions.[11,14,16]

The uptake probability of HOBr on KBr substrates at low flow rate is surprisingly high. Beichert et al. argued for a relation between the accommodation coefficient α and the uptake probability γ with respect to strongly adsorbed water in the case of the reaction of HNO_3 with solid NaCl:[18]

$$HNO_3 \underset{k_{evap}}{\overset{\alpha}{\rightleftharpoons}} HNO_3(ads.) \xrightarrow{k_{rxn}} \text{products}$$

This relation is simply expressed as $\gamma = \alpha[k_{rxn}/(k_{rxn} + k_{evap})]$, where k_{rxn} is the rate of heterogeneous reaction and k_{evap} is the rate of reevaporation of adsorbed HNO_3. Thus, for the interaction of a gas-phase species at the interface between two different phases, the accommodation coefficient α represents the upper limit of the uptake probability γ. However, there does not exist an a priori value of the accommodation coefficient

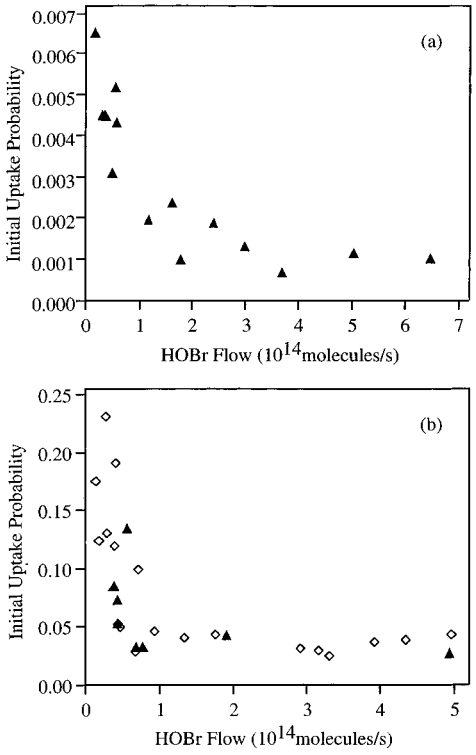

Figure 5. Initial uptake probabilities of HOBr reacting on (a) NaCl and (b) KBr substrates as a function of the HOBr flow rate in the 14 mm orifice reactor. Uptake probabilities on powder substrates (triangles) are obtained by calculating the correction factor for powder substrates according to the pore diffusion model of Keyser et al. Results on spray-deposited substrates are presented as diamonds.

TABLE 2: Steady-State Experiments on NaCl[a,b]

type	flow, molecules/s	mass, g	k_{uni}, s^{-1}	γ_{obs}	γ_{tr}
powder	2.1×10^{13}	>10	3.56	5.1×10^{-2}	6.5×10^{-3}
powder	3.4×10^{13}	>10	2.79	4.0×10^{-2}	4.5×10^{-3}
powder	3.7×10^{13}	>10	2.90	4.2×10^{-2}	4.5×10^{-3}
powder	4.0×10^{13}	>10	2.78	4.0×10^{-2}	4.4×10^{-3}
powder	5.1×10^{13}	>10	2.32	3.4×10^{-2}	3.1×10^{-3}
powder	5.7×10^{13}	>10	3.13	4.5×10^{-2}	5.1×10^{-3}
powder	5.9×10^{13}	>10	2.79	4.0×10^{-2}	4.3×10^{-3}
powder	1.2×10^{14}	>10	1.82	2.6×10^{-2}	1.9×10^{-3}
powder	1.6×10^{14}	>10	1.97	2.8×10^{-2}	2.3×10^{-3}
powder	1.8×10^{14}	>10	1.20	1.7×10^{-2}	9.7×10^{-4}
powder	2.4×10^{14}	>10	1.73	2.5×10^{-2}	1.9×10^{-3}
powder	3.0×10^{14}	>10	1.35	2.0×10^{-2}	1.3×10^{-3}
powder	3.7×10^{14}	>10	1.00	1.4×10^{-2}	6.5×10^{-4}
powder	5.1×10^{14}	>10	1.33	1.9×10^{-2}	1.1×10^{-3}
powder	6.5×10^{14}	>10	1.22	1.8×10^{-2}	9.9×10^{-4}
grain	5.8×10^{13}	1.11	0.70	1.1×10^{-2}	2.8×10^{-3}
grain	5.8×10^{13}	2.01	1.32	1.9×10^{-2}	2.8×10^{-3}
grain	5.8×10^{13}	3.31	1.74	2.5×10^{-2}	2.8×10^{-3}
grain	5.8×10^{13}	4.48	1.96	2.8×10^{-2}	2.8×10^{-3}
grain	5.8×10^{13}	7.01	2.01	2.9×10^{-2}	2.8×10^{-3}

[a] More than 10 g of NaCl is used for all experiments using powder substrates in order to measure γ_{obs} at the asymptote of the conversion function displayed in Figure 2. Grain substrates have characteristic dimensions in the range 350−500 μm. [b] From the scatter of the uptake probabilities displayed in Figure 5 we deduce a random (statistical) error of γ of a factor of 2 for HOBr flow rates $\geq 1 \times 10^{14}$ molecules s^{-1} and assert that any systematic error is smaller than the stated random error. This uncertainty matches the signal-to-noise ratio of the individual determinations of γ down to the smallest signal intensities. The given random error leads to a value of γ extrapolated to vanishing flow rate of HOBr of $\leq(6.5 \pm 2.5) \times 10^{-3}$ for NaCl substrates.

of HOBr on salt so that it becomes difficult to prove the above relation. Sander and Crutzen[23] presented a model calculation for the marine boundary layer in which they take into account

TABLE 3: Steady-State Experiments on KBr[a,b]

type	flow, molecules/s	mass, g	k_{uni}, s^{-1}	γ_{obs}	γ_{tr}
powder	3.9×10^{13}	>10	21.3	0.309	8.4×10^{-2}
powder	4.4×10^{13}	>10	19.2	0.278	7.2×10^{-2}
powder	4.4×10^{13}	>10	15.2	0.220	5.1×10^{-2}
powder	5.7×10^{13}	>10	30.0	0.434	1.3×10^{-2}
powder	6.9×10^{13}	>10	10.9	0.158	3.1×10^{-2}
powder	7.8×10^{13}	>10	11.0	0.159	3.1×10^{-2}
powder	1.9×10^{14}	>10	13.2	0.191	4.2×10^{-2}
powder	4.9×10^{14}	>10	9.53	0.134	2.5×10^{-2}
spray	1.4×10^{13}		12.1	0.18	0.18
spray	1.7×10^{13}		8.56	0.12	0.12
spray	2.6×10^{13}		16.0	0.23	0.23
spray	2.9×10^{13}		9.00	0.13	0.13
spray	3.9×10^{13}		8.25	0.12	0.12
spray	4.0×10^{13}		13.2	0.19	0.19
spray	4.4×10^{13}		3.62	5.2×10^{-2}	5.2×10^{-2}
spray	4.6×10^{13}		3.43	5.0×10^{-2}	5.0×10^{-2}
spray	6.6×10^{13}		1.98	2.9×10^{-2}	2.9×10^{-2}
spray	7.0×10^{13}		6.82	9.9×10^{-2}	9.9×10^{-2}
spray	9.3×10^{13}		3.15	4.6×10^{-2}	4.6×10^{-2}
spray	1.3×10^{14}		2.79	4.0×10^{-2}	4.0×10^{-2}
spray	1.8×10^{14}		3.00	4.3×10^{-2}	4.3×10^{-2}
spray	2.9×10^{14}		2.15	3.1×10^{-2}	3.1×10^{-2}
spray	3.2×10^{14}		2.04	3.0×10^{-2}	3.0×10^{-2}
spray	3.3×10^{14}		1.69	2.4×10^{-2}	2.4×10^{-2}
spray	3.9×10^{14}		2.54	3.7×10^{-2}	3.7×10^{-2}
spray	4.3×10^{14}		2.65	3.8×10^{-2}	3.8×10^{-2}
spray	5.0×10^{14}		2.99	4.3×10^{-2}	4.3×10^{-2}
spray	7.8×10^{14}		4.25	6.2×10^{-2}	6.2×10^{-2}
spray	9.1×10^{14}		4.46	6.4×10^{-2}	6.4×10^{-2}

[a] More than 10 g of KBr is used for all experiments using powder substrates in order to measure γ_{obs} at the asymptote of the conversion function displayed in Figure 2. [b] From the scatter of the uptake probabilities displayed in Figure 5 we deduce a random (statistical) error of γ of a factor of 2 for HOBr flow rates $\geq 1 \times 10^{14}$ molecules s^{-1} and assert that any systematic error is smaller than the stated random error. This uncertainty matches the signal-to-noise ratio of the individual determinations of γ down to the smallest signal intensities. The given random error leads to a value of γ extrapolated to vanishing flow rate of HOBr of $\leq 0.18 \pm 0.04$ for KBr substrates.

the effect of deliquescent sea salt aerosol particles. They used an estimated accommodation coefficient α of 0.056 for the interaction of HOBr on a liquid salt solution regardless of composition or ion content. However, in the present case the observed γ is significantly larger than the cited α, at least for solid bromide (see Table 3) which puts serious doubt as to the validity of their choice for α, even when considering the difference between the condensed phase and the solid surface. In all likelihood α must be equal to or larger than the upper limit of γ_{tr} ($=0.18 \pm 0.04$) in order for it to qualify as a mass accommodation coefficient.

The two types of salt samples, namely, the powder substrates and the spray-deposited substrates, were placed into the Knudsen reactor and evacuated until the partial pressure of water dropped to the background level of approximately 10^{-6} Torr. Sometimes we intentionally measured the HOBr uptake on salt substrates containing an increased amount of H_2O vapor at a partial pressure between 10^{-3} and 10^{-4} Torr by (1) minimizing the pumping time and (2) introducing a flow of H_2O vapor into the Knudsen cell reactor. In both cases, no systematic change of the uptake probability of HOBr on salt was ever observed. Similarly to the analoguous aqueous phase reactions the presence of adsorbed water on salt enables the present type of reactions via ionic displacement processes. The negative experimental results involving added H_2O vapor means that there already are sufficient quantities of strongly adsorbed H_2O on the present salt samples. Even though H_2O does not appear in the stoichiometric balance, it is an essential reagent enabling the

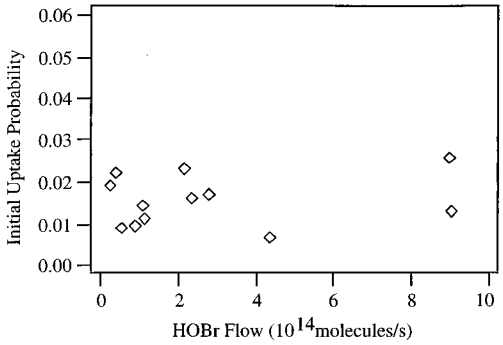

Figure 6. Initial uptake probability of the HOBr reaction on $NaNO_3$ spray-deposited substrates as a function of the HOBr flow rate. The 14 mm orifice was used.

reactions under study. The quantity of this strongly adsorbed H_2O amounts to between 10 and 20 molecular monolayers for spray-deposited NaCl substrates at our experimental conditions[14] and has been called the quasi-liquid layer (QLL) by Beichert and Finlayson-Pitts.[18] In summary, the experiments involving H_2O vapor have shown that (1) there is H_2O vapor which is strongly adsorbed on thin film salt substrates despite having dried the samples under vacuum of the order of 10^{-6} Torr for up to several days and (2) the quantities are on the order of tens of monolayers for spray-deposited NaCl samples. Therefore, we expect that the chemical reactions taking place on those solid crystalline samples under laboratory conditions are not too different from those occurring on humid salt aerosols.

HOBr Self-Reaction. It is unexpected that Br_2 is released from the HOBr reaction with NaCl. A possible explanation is that BrCl is converted into Br_2 heterogeneously according to the following reaction.

$$2BrCl \rightarrow Br_2 + Cl_2 \qquad (17)$$

However, we have not observed Cl_2 in cases where we have observed Br_2 so that reaction 17 may not take place under our conditions.

Another explanation would be that a small amount of Br containing impurity in NaCl such as NaBr reacts with HOBr and produces Br_2 competitively. To clarify the origin of Br_2, we tested the reactivity of HOBr on $NaNO_3$, which is a non-halogen containing salt. In steady-state experiments, Br_2 appears just after opening the sample chamber by lifting the plunger, similar to the reaction of HOBr with NaCl and KBr. Since the Br impurity in $NaNO_3$ is negligible, all bromine atoms of Br_2 released must originate from bromine atoms in HOBr. This result indicates that a HOBr self-reaction occurs on salt surfaces and releases Br_2. Figure 6 shows the initial uptake probabilities of HOBr reacting on $NaNO_3$ spray-deposited substrates as a function of the HOBr flow rate. This rate of HOBr self-reaction on $NaNO_3$ is large enough to explain the rate of Br_2 formation on NaCl surfaces exclusively by this mechanism. By inference we assume that for the HOBr/KBr heterogeneous reaction part of the Br_2 also comes from the HOBr self-reaction.

The ratio of Br_2 molecules released to HOBr molecules taken up measured as a function of flow rate is shown in Figure 7. This plot obtains the yield of the heterogeneous decomposition of HOBr on solid $NaNO_3$. The yields are obtained after 20 and 35 s exposure, respectively. The obtained values are approximately 50% and found to be independent of the HOBr flow rate. Thus, one Br_2 molecule desorbed corresponds to two HOBr molecules adsorbed over the whole range of the HOBr flow. The 50% yield supports the hypothesis of the HOBr self-

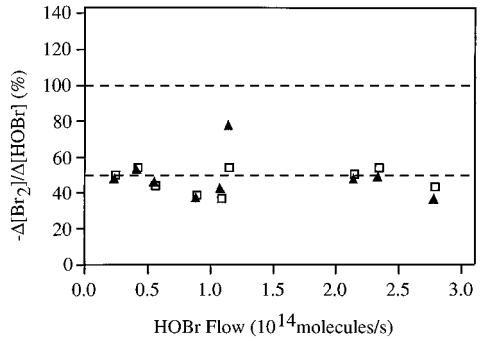

Figure 7. Br_2 yields of the reaction of HOBr with $NaNO_3$ spray-deposited substrates. The 14 mm orifice was used. Diamonds: Yield after 20 s exposure. Squares: Yield after 35 s exposure.

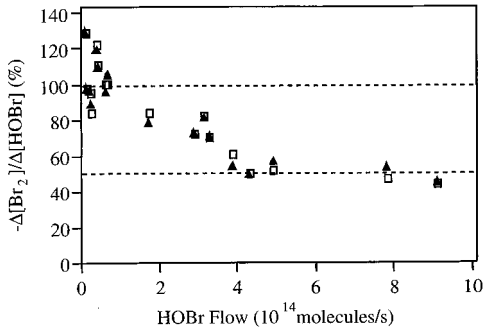

Figure 8. Br_2 yields of the reaction of HOBr with KBr spray-deposited substrates. The 14 mm orifice was used. Diamonds: Yield after 20 s exposure. Squares: Yield after 35 s exposure.

reaction according to the net reaction

$$2HOBr \rightarrow Br_2 + {}^1/_2O_2 + H_2O \qquad (18)$$

The self-reaction of HOBr has been suggested before in the uptake of HOBr on ice[30,33] and on sulfuric acid.[32,50] In all of these reports it is suggested that the self-reaction of HOBr produces Br_2O according to equilibrium 11. However, in our experiments of HOBr reacting on salt surfaces we never observed an increase in Br_2O monitored at *m*/*e* 176 (Br_2O^+, see Figures 3a and 4a). We therefore conclude that either the self-reaction of HOBr on salt does not lead to Br_2O at all or it decomposes in a fast reaction according to reaction 18 or quickly reacts with the salt substrate. The facts that HOBr decomposes on $NaNO_3$ without formation of Br_2O, that the Br_2 yield is 50%, and that the rate of decomposition is similar to the one observed for HOBr reaction on solid alkali metal salt substrates are seen as strong evidence for reaction 18 on solid alkali metal salts. Thus, HOBr adsorbed either on alkali metal halide salts or on neutral or acidic ice surfaces behaves differently.

The yield measurements are also performed for the reaction of HOBr with KBr substrates. Figure 8 shows the yield of Br_2 per HOBr taken up for the reaction of HOBr with KBr spray-deposited substrates. Spray-deposited substrates instead of the powder substrates had to be used for this yield measurement because we observed a slight nonreactive adsorption of Br_2 on the salt surface and subsequent diffusion of Br_2 into the interstitial void of the salt sample, thus lowering the observed yield of Br_2.

The residence time of Br_2 on the salt surfaces or in the Knudsen cell reactor affects the measurement of Br_2 yields in case the residence time is longer than the time scale for the decay of HOBr due to uptake because we compare the rate of disappearance of HOBr and the rate of appearance of Br_2 at the same time. As seen in Figure 4, pulsed-valve experiments using the 14 mm orifice shows that the Br_2 signal peaks at a time on the order of 100 ms. A delay on the order of 100 ms is short enough to compare the disappearance of HOBr and the appearance of Br_2 because the lifetime of HOBr due to uptake is between several seconds and several tens of seconds. Thus, we conclude that the residence time of Br_2 does not affect the Br_2 yields under our experimental conditions.

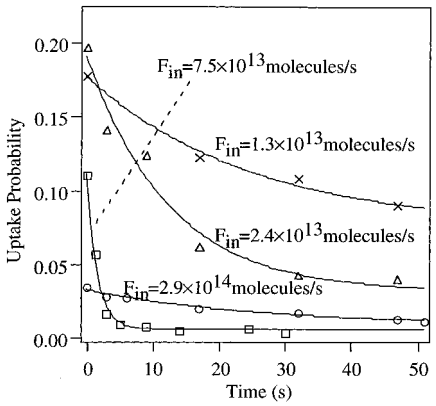

Figure 9. Uptake probabilities γ of HOBr reacting on KBr spray-deposited substrates at several flow rates as a function of time. These results show the large sensitivity of γ_0 to the HOBr flow rate.

Figure 8 shows that the yield of Br_2 is 100% at low flow rate and 50% at high flow rate. This means that the HOBr reaction with KBr is dominant at low flow rate, whereas at high flow rate the HOBr self-reaction is dominant. This would relegate the HOBr self-reaction into the realm of a laboratory curiosity compared to atmospheric conditions with the extremely low vapor pressures of HOBr (on the order of 10^8 molecules cm^{-3}) which thus strongly favors reactions 14 and 16 as opposed to reaction 18. It is clear that there is a characteristic difference between the flow rate dependence of the initial uptake probability on NaCl and KBr shown in Figure 5 and that on $NaNO_3$ in Figure 6. In contrast to the results on NaCl and KBr substrates, there seems to be no dependence of γ on the HOBr flow rate in our measured range for the self-reaction of HOBr on $NaNO_3$. It is quite likely that the competition of both reactions is in part responsible for the flow rate dependence of the initial uptake probability on NaCl and KBr, as shown in Figure 5.

Yield measurements of the HOBr reaction with NaCl using spray-deposited substrates over a wide range of HOBr flows were not possible because the production of BrCl and Br_2 is not measurable. A few experiments have nevertheless been performed using the 8 mm orifice for a HOBr flow rate in the range $(2-5) \times 10^{13}$ molecules/s at which flows uptake probabilities are large enough to observe both BrCl and Br_2. This measurement reveals a branching ratio of BrCl to Br_2 of approximately 2:1. Taking into account that the self-reaction of HOBr resulting in Br_2 is less important at low flow rates in the case of the HOBr reaction with KBr, the heterogeneous reaction of HOBr with NaCl to result in BrCl may be important under atmospheric conditions of low partial pressures of HOBr.

Surface Saturation. Figure 9 shows the uptake probability of HOBr on KBr spray-deposited samples as a function of time at several flow rates. As discussed above, we concluded that at low flow rate the heterogeneous reaction of HOBr with KBr is dominant, whereas the self-reaction becomes increasingly important at increasing flow rate. The rapid saturation of the

initial uptake at low concentrations of HOBr gives an indication of how many Br atoms on the surface are capable of reacting with adsorbed HOBr molecules. The total geometric area of the surface is 1.96×10^{15} nm^2 (19.6 cm^2; see Table 1), and the difference to the real surface area has been reported to be within a factor of 2.[14] The interatomic distance of K−Br is 0.33 nm, which means that one Br atom occupies a surface area of 0.22 nm^2 on a crystalline KBr surface. Thus, the number of Br atoms on the total geometric sample surface is estimated to be approximately $(1-2) \times 10^{16}$. At the low flow rate of HOBr of $F_{in} = 1.3 \times 10^{13}$ molecules/s (see Figure 9), a large part of the injected HOBr interacts with salt, thus leading to a surface reaction rate of approximately 1×10^{13} molecules/s. As is seen in Figure 9, the time during which the uptake probability drops to half of its initial value is about 50 s for $F_{in} = 1.3 \times 10^{13}$ molecules/s. We assume that the uptake probability is proportional to the remaining number of bromine atoms which can react with HOBr. After 50 s 5×10^{14} molecules have reacted which would indicate that twice that number, namely, 1×10^{15} Br atoms, were capable of undergoing a heterogeneous reaction with HOBr. This leads to the conclusion that approximately 5−10% of all bromine atoms on the surface are involved in the reaction.

Atoms at surface defects such as ridges and kinks may be more reactive than on an ideal flat surface. Therefore, one hypothesis is that the heterogeneous reaction takes place at defect sites. However, we also have to take into account the presence of strongly bound water on the salt surface as briefly discussed above. We measured the amount of surface bound water in an experiment where the salt surface was placed for several days under vacuum at pressures less than 10^{-6} Torr until the MS signal of H_2O disappeared. Subsequently the surface was heated to approximately 500 K in the high-temperature sample support to result in an integrated H_2O MS signal corresponding to 10−20 formal monolayers desorbing from the surface. Thus, in our pressure range ($<10^{-3}$ Torr), at least 10 molecular layers of H_2O may remain adsorbed at the interface. Surface studies of adsorbed H_2O resulted in an ordered two-dimensional array of H_2O molecules on a perfectly flat surface.[51−53] Therefore, at most only one monolayer of H_2O covers the surface and the remainder probably accumulates on defect sites. It is probable that the ionic reaction of HOBr with Br^- or Cl^- occurs in the bulk liquid preferentially accumulated on surface defects. This scenario is consistent with the conclusions regarding heterogeneous reactions on salt which require some amount of adsorbed water in order to proceed, even at as low a pressure as was used in this study. This requirement has been documented recently by Beichert and Finlayson-Pitts[18] and Fenter et al.[14]

One may argue that the decrease of the uptake at high flow rates as seen in Figure 9 is due to the effect of fast surface saturation processes. At a HOBr flow rate of $F_{in} = 2.4 \times 10^{13}$ molecules/s, the half-life $\tau_{1/2}$ to reach steady-state uptake is approximately 15 s. When we consider a HOBr flow rate higher by a factor of 10 ($F_{in} = 2.9 \times 10^{14}$ molecules/s; cf. Figure 9) and assume that the rate of occupation of active sites is proportional to the HOBr partial pressure, the lifetime for the decrease of γ is estimated to be approximately 2 s.[54] However, we do not observe any fast saturation process for the highest HOBr flow rate displayed in Figure 9 and believe that a decay within 2 s should still be observable because the residence time of HOBr in the Knudsen reactor and the time constant of the used amplifier are both much smaller. We therefore believe that the mechanism of the heterogeneous interaction of HOBr with solid KBr may change at high concentrations of HOBr because no sign of the expected fast saturation of γ has been observed.

Consistent with this changeover of the mechanism for the heterogeneous reaction of HOBr on salt are the results on the Br_2 yields displayed in Figure 8 which point to the increasing role of surface-induced self-reaction at flow rates F_{in} in excess of 1×10^{14} molecules/s. Furthermore, the buildup of the involatile bases NaOH and KOH resulting from the interaction of HOBr on solid salts according to reactions 14 and 16 may well be responsible for the fast saturation of the HOBr uptake reaction. This fast saturation displayed both in Figures 5 and 9 is compounded by the fact that only 5−10% of the external surface is reactive. In addition, the buildup of involatile bases may also be responsible for the slow decrease of γ with time which has been observed at higher flow rates of HOBr, typically 2.9×10^{14} molecules/s (Figure 9).

Atmospheric Importance. Although there are no observations of HOBr in the atmosphere, its concentration is predicted to reach values between one to several tens of pptv in the troposphere and in the stratosphere. Our study revealed that HOBr has a potential to react with dry and wet sea salt aerosol in the troposphere and with salt aerosol after volcanic eruptions in the stratosphere according to reactions 14 and 16. The

$$\mathrm{HOBr + NaCl(s) \rightarrow BrCl + NaOH(s)} \qquad (14)$$

$$\mathrm{HOBr + KBr(s) \rightarrow Br_2 + KOH(s)} \qquad (16)$$

resulting BrCl and Br_2 undergo photolysis to produce active halogen atoms which cause ozone destruction and oxidation of hydrocarbons. Sander and Crutzen[23] calculated photolysis rates of Br_2 and BrCl of 2.0×10^{-2} and 5.9×10^{-3} s^{-1} in the troposphere. Since the photolysis of HOBr results in OH and Br at a rate of $J = 3.5 \times 10^{-4}$ s^{-1} in the troposphere, these heterogeneous reactions on salts effectively convert OH radicals into halogen atoms. The importance of these reactions lies in the fact that two halogen atoms are released into the gas phase per HOBr consumed and thus increases the halogen atom concentration in the atmosphere by converting an (inactive) halide into an active halogen atom by consuming a OH free radical.

The crucial question is whether the heterogeneous reaction 14 or 16 is competitive with the photolysis frequency of HOBr given above for the troposphere. We assume a typical salt aerosol particle radius of $r = 10^{-4}$ cm (1 μm) and a mass number density N of 10 particles cm^{-3} leading to 1.26×10^{-6} cm^2 cm^{-3} (126 μm^2 cm^{-3}). The first-order mass transfer rate constant k_{mt} is calculated as 1.26×10^{-3} s^{-1} according to the approximation $k_{mt} = 4\pi rDN$ with D being the diffusion coefficient in 1 atm of air at ambient temperature ($D = 0.1$ cm^2 s^{-1}). The first-order interfacial rate constants k_{het} for HOBr interacting with NaCl and KBr are 5.2×10^{-5} and 1.44×10^{-3} s^{-1}, respectively, when we use the uptake coefficients at limiting low flow rates and ambient temperature obtained in this work, namely, $\gamma = 6.5 \times 10^{-3}$ and 0.18 for NaCl and KBr, respectively. For the heterogeneous reaction of HOBr on NaCl the interfacial rate process is rate limiting, whereas for the faster reaction on KBr both k_{mt} and k_{het} are about equal. The combined rate constant k_{tot} is computed from the law of combination of kinetic resistances and amounts to 6.7×10^{-4} and 5.0×10^{-5} for KBr and NaCl, respectively. It is apparent that the heterogeneous reaction of HOBr on KBr is competitive with photolysis in the troposphere, whereas for NaCl the branching

ratio between photolysis and heterogeneous reaction is about seven to one at the chosen aersol loading typical of the remote marine boundary layer.

We have semiquantitatively assessed the importance of these heterogeneous reactions in the stratosphere using the volcanic eruption of El Chichon as an example. Following an approximation described by Michelangeli et al.,[55] the rate of loss of HOBr in the presence of volcanic NaCl aerosol is $J_{NaCl} = 6.7 \times 10^{-5}$ s^{-1} using the observed uptake probability of $\gamma = 6.5 \times 10^{-3}$ for reaction 14 at a limiting low flow rate of HOBr. Although this rate is roughly 10 times lower than HOBr photolysis in the stratosphere,[56] it is fast enough to significantly affect the total chlorine density in competition with photolysis. At night heterogeneous chemistry of HOBr is thought to be the dominant loss process.

Another implication of potential importance under atmospheric conditions is the fact that HOBr may decompose heterogeneously. As seen in Figure 6, we observed the uptake of HOBr on $NaNO_3$ at a flow rate of 1×10^{13} molecules s^{-1}, which corresponds to approximately 1×10^9 molecules/cm^3. Although the HOBr density in the atmosphere may be roughly 10 times lower than the above value, the constant uptake probability displayed in Figure 6 implies that decomposition of HOBr may take place on surfaces such as mineral dust. This decomposition would reduce the radical density as two OH free radicals would effectively be consumed.

Conclusions

We have measured the HOBr uptake kinetics on solid NaCl and KBr for the first time. Both BrCl and Br_2 are the observed products for the reaction of HOBr with NaCl, whereas Br_2 was the sole product of the reaction of HOBr on KBr. The uptake probability of HOBr on NaCl and KBr depends on the HOBr concentration in the gas phase, and uptake probabilities $\gamma_0 \leq (6.5 \pm 2.5) \times 10^{-3}$ for NaCl and $\gamma_0 \leq 0.18 \pm 0.04$ for KBr are obtained at ambient temperature under our experimental conditions. The production of Br_2 from HOBr was observed even on NaCl and non-halogen containing ionic substrates such as $NaNO_3$. This behavior is interpreted in terms of a HOBr self-reaction which produces Br_2 according to the reaction $2HOBr \rightarrow Br_2 + {}^1/_2O_2 + H_2O$. For KBr substrates, there is competition between the HOBr reaction with KBr and the HOBr self-reaction which is favored at the upper partial pressure range used in our experiments. The lifetime of the surface saturation process indicates that HOBr reacts with alkali metal halides on a limited number of reactive sites on the salt surface of the order of 5−10%.

Acknowledgment. Funding for this work was provided by Avina Foundation in the framework of the "Alliance for Global Sustainability" (AGS) and Office Fédéral de l'Education et de la Science (OFES) as part of the European subproject HALOTROP. We thank F. Caloz, A. Aguzzi, R. Oppliger, and A. Allanic for their assistance in the experiments.

References and Notes

(1) Barrie, L. A.; Bottenheim J. W.; Schnell R. C.; Crutzen P. J.; Rasmussen R. A. *Nature* **1988**, *334*, 138.

(2) Bottenheim, J. W.; Barrie, L. A.; Atlas, E.; Heidt, L. E.; Niki, H.; Rasmussen, R. A.; Shepson, P. B. *J. Geophys. Res.* **1988**, *95*, 18555.

(3) Hausmann, M.; Platt, U. *J. Geophys. Res.* **1994**, *99*, 25399.

(4) Li, S.-M.; Yokouchi, Y.; Barrie, L. A.; Muthuramu, K.; Shepson, P. B.; Bottenheim, J. W.; Sturges, W. T.; Landsberger, S. *J. Geophys. Res.* **1994**, *99*, 25415.

(5) Solberg, S.; Schmidbauer, N.; Semb, A.; Stordal, F.; Hov, Ø. *J. Atmos. Chem.* **1996**, *23*, 301.

(6) Impey, G. A.; Shepson, P. B.; Hastie, D. R.; Barrie, L. A. *J. Geophys. Res.* **1997**, *102*, 16005.

(7) Schroeder, W. H.; Urone, P. *Environ. Sci. Technol.* **1974**, *8*, 756.

(8) Finlayson-Pitts, B. J. *Nature* **1983**, *306*, 676.

(9) George, C.; Ponche, J. L.; Mirabel, P.; Behnke, W.; Scheer, V.; Zetzsch, C. *J. Phys. Chem.* **1994**, *98*, 8780.

(10) Vogt, R.; Finlayson-Pitts, B. J. *J. Phys. Chem.* **1994**, *98*, 3747.

(11) Fenter, F. F.; Caloz, F.; Rossi, M. J. *J. Phys. Chem.* **1994**, *98*, 9801.

(12) Timonen, R. S.; Chu, L. T.; Leu, M.-T.; Keyser, L. F. *J. Phys. Chem.* **1995**, *99*, 9509.

(13) Leu, M.-T.; Timonen, R. S.; Keyser, L. F. *J. Phys. Chem.* **1995**, *99*, 13203.

(14) Fenter, F. F.; Caloz, F.; Rossi, M. J. *J. Phys. Chem.* **1996**, *100*, 1008.

(15) Allen, H. C.; Laux, J. M.; Vogt, R.; Finlayson-Pitts, B. J.; Hemminger J. C. *J. Phys. Chem.* **1996**, *100*, 6371.

(16) Caloz, F.; Fenter, F. F.; Rossi, M. J. *J. Phys. Chem.* ***1996***, *100*, 7494.

(17) Peters, S. J.; Ewing, G. E. *J. Phys. Chem.* **1996**, *100*, 14093.

(18) Beichert, P.; Finlayson-Pitts, B. J. *J. Phys. Chem.* **1996**, *100*, 15218.

(19) Laux, J. M.; Fister, T. F.; Finlayson-Pitts, B. J.; Hemminger, J. C. *J. Phys. Chem.* **1996**, *100*, 19891.

(20) Behnke, W.; George, C.; Scheer, V.; Zetzsch, C. *J. Geophys. Res.* **1997**, *102*, 3795.

(21) Seisel, S.; Caloz, F.; Fenter, F. F.; van den Bergh, H.; Rossi, M. *J. Geophys. Res. Lett.* **1997**, *24*, 2757.

(22) Fan, S.-M.; Jacob, D. J. *Nature* **1992**, *359*, 522.

(23) Sander, R.; Crutzen, P. J. *J. Geophys. Res.* **1995**, *101*, 9121.

(24) Vogt, R.; Crutzen, P. J.; Sander, R. *Nature* **1996**, *383*, 327.

(25) Tang, T.; McConnell, J. C. *Geophys. Res. Lett.* **1996**, *23*, 2633.

(26) McGrath, M. P.; Rowland, F. S. *J. Phys. Chem.* **1994**, *98*, 4773.

(27) Orlando, J. J.; Burkholder, J. B. *J. Phys. Chem.* **1995**, *99*, 1143.

(28) Lock, M.; Barnes, R. J.; Sinha, A. *J. Phys. Chem.* **1996**, *100*, 7972.

(29) Francisco, J. S.; Hand, M. R.; Williams, I. H. *J. Phys. Chem.* **1996**, *100*, 9250.

(30) Abbatt, J. P. D. *Geophys. Res. Lett.* **1994**, *21*, 665.

(31) Allanic, A.; Oppliger, R.; Rossi, M. J. *J. Geophys. Res.* **1997**, *102*, 23529.

(32) Abbatt, J. P. D. *J. Geophys. Res.* **1995**, *100*, 14009.

(33) Kirchner, U.; Benter, Th.; Schindler, R. N. *Ber Bunsen-Ges. Phys. Chem.* **1997**, *101*, 975.

(34) Woods, D. C.; Chaun, R. L.; Rose W. I. *Science* **1985**, *230*, 170.

(35) Cahill, T. A.; Wilkinson, K.; Schnell , R. *J. Geophys. Res.* **1992**, *97*, 14513.

(36) Parungo, F.; Kopcewicz, B.; Nagamoto, C.; Schnell, R.; Sheridan, P.; Zhu, C.; Harris, J. *J. Geophys. Res.* **1992**, *97*, 15867.

(37) Lowenthal, D. H.; Borys, R. D.; Rogers, C. F.; Chow, J. C.; Stevens, R. K.; Pinto, J. P.; Ondov, J. M. *Geophys. Res. Lett.* **1993**, *20*, 693.

(38) Shaw, G. E. *J. Geophys. Res.* **1991**, *96*, 22369.

(39) Caloz, F.; Fenter, F. F.; Tabor, K. D.; Rossi, M. J. *Rev. Sci. Instrum.* **1997**, *68*, 3172.

(40) Fenter, F. F.; Caloz, F.; Rossi, M. J. *Rev. Sci. Instrum.* **1997**, *68*, 3180.

(41) Keyser, L. F.; Moore, S. B.; Leu, M.-T. *J. Phys. Chem.* **1991**, *95*, 5496.

(42) Chu, L. T.; Leu, M.-T.; Keyser, L. F. *J. Phys. Chem.* **1993**, *97*, 12798.

(43) Chu, L. T.; Leu, M.-T.; Keyser, L. F. *J. Phys. Chem.* **1993**, *97*, 7779.

(44) Keyser, L. F.; Leu, M.-T.; Moore, S. B. *J. Phys. Chem.* **1993**, *97*, 2800.

(45) Keyser, L. F.; Leu, M.-T. *J. Colloid Interface Sci.* **1993**, *155*, 137.

(46) Wheeler, A. *Adv. Catal.* **1951**, *3*, 249.

(47) Aris, R. *The Mathematical Theory of Diffusion and Reaction in Permeable Catalysis*; Clarendon Press: Oxford, U.K., 1975; Vol. I.

(48) Dahneke, B. In *Theory of Dispersed Multiphase Flow*; Meyer, R. E., Ed.; Academic Press: New York, 1983; p 97.

(49) Fitzgerald, J. M. *Atmos. Environ.* **1991**, *25A*, 533.

(50) Hanson, D. R.; Ravishankara, A. R.; Lovejoy, E. R. *J. Geophys. Res.* **1996**, *101*, 9063.

(51) Fölsh, S.; Stock A.; Henzler M. *Surf. Sci.* **1992**, *264*, 65.

(52) Tepper, P.; Zink, J. C.; Schmelz, H.; Wassermann, B.; Reif, J.; Matthias, E. *J. Vac. Sci. Technol.* **1989**, *B7*, 1212.

(53) Fölsh, S.; Henzler M. *Surf. Sci.* **1991**, *247*, 269.

(54) At a HOBr flow rate of 2.9×10^{14} molecules/s the concentration in the Knudsen reactor before reaction is 5.0×10^{10} molecules cm^{-3} (N_{coll}-(nr)), leading to 6.3×10^{15} collisions s^{-1} on the total geometric surface area of the sample. Assuming an upper limit of $\gamma = 0.18$, the concentration of HOBr and the total collision frequency during the reaction are reduced to 1.0×10^{10} molecules cm^{-3} and 1.3×10^{15} collisions s^{-1} ($N_{coll}(r)$), respectively, resulting in an absolute uptake rate of 2.3×10^{14} molecules

s^{-1} ($=\gamma N_{coll}(r)$). With a number of 1×10^{15} Br atoms available for reaction on the total sample surface, the half-life of the substrate is on the order of several seconds.

(55) Michelangeli, D. V.; Allen, M.; Yung, Y. L. *Geophys. Res. Lett*. **1991**, *18*, 673.

(56) DeMore, W. B.; Sander, S. P.; Golden, D. M.; Hampson, R. F.; Kurylo, M. J.; Howard, C. J.; Ravishankara, A. R.; Kolb, C. E.; Molina, M. J. *Chemical Kinetics and Photochemical Data for Use in Stratospheric Modeling*; JPL Publication 97-4; NASA. Jet Propulsion Laboratory: Pasadena, CA 1997.